

Identification of 13 Cepheids and 333 Other Variables in M31

Y. C. Joshi¹, A. K. Pandey¹, D. Narasimha², R. Sagar¹ and Y. Giraud-Héraud³

¹ State Observatory, Manora peak, Naini Tal - 263129, Uttarakhand, India

² Tata Institute of Fundamental Research, Homi Bhabha Road, Mumbai – 400 005, India

³ Laboratoire de Physique Corpusculaire, Collège de France, Laboratoire associé au CNRS-IN2P3 (URA 6411),
11 place Marcelin Berthelot, 75231 Paris Cedex 05, France

Received — / accepted —

Abstract. We present Cousins R and I band photometry of variable stars in a $\sim 13' \times 13'$ region in the disk of M31 galaxy, obtained during 141 nights. Of the 26 Cepheid variables present in the region, two are newly discovered, 11 are classified as Cepheids for the first time and 13 are confirmed as Cepheids. The extensive photometry of these Cepheids enabled us to determine precise phase and amplitude of pulsation which ranges from 0.11 to 0.48 mag in R band. The period of variability ranges from ~ 7.5 to 56 days. The period-luminosity diagram is used to derive a distance modulus of 24.49 ± 0.11 mag for M31 galaxy. We also report variability in 333 other stars, of them, 115 stars appear to be long period variables, 2 suspected eclipsing binaries and remaining 216 are irregular variables.

Key words. Cepheids – variable stars – M31 Galaxy – photometry

1. Introduction

In recent years, the Andromeda galaxy (M31) has been a target of search for gravitational microlensing events (Crofts & Tomaney 1996, Ansari et al. 1997). To detect lensing events, continuous observations are needed for a long duration though for a short period of time each night. Such observations are, therefore, very useful to search for variable stars (e.g. Cepheids, Miras) also. The catalogues of variable stars compiled from such a monitoring programme are generally complete within the flux limitation, because of the continuous observation of the same field over a long period. Various groups (e.g. MACHO, EROS, OGLE) dedicated to search for microlensing events in the Galactic Bulge and Magellanic Clouds have already identified a large number of variable stars as a bi-product (Welch et al. 1997, Udalski et al. 1999a) and the catalogues of Cepheid variables brought out by these projects (Beaulieu et al., 1995, Udalski et al. 1999b) have given insight into the pulsation properties of Cepheids.

In collaboration with the AGAPE (Andromeda Gravitational Amplification Pixel Experiment) group, we started Cousins R and I photometric observations of M31 in 1998 with an aim to search for microlensing events. Based on the observations of first 2 years, Joshi et al. (2001, hereafter referred as paper I) reported 8 variables, 7 of them were suspected as Cepheids and one Mira-like

variable. In this paper, we extended our analysis to detect the variable stars using four years of observations. Details of our observations are given in next section while Sect. 3 outlines the detailed photometry of our data. The detection of variable stars is described in Sect. 4 which leads to discovery of some new Cepheids. The catalogue of Cepheids, their period-luminosity relation, colour-magnitude diagram along with a brief discussion of some of the Cepheids are presented in Sect. 5. Other type of variables along with discussion and conclusion are given in the remaining part of the paper.

2. Observation and image processing

The Cousins R and I broad band photometric observations were carried out at the f/13 Cassegrain 104-cm Sampurnanand Telescope of the State Observatory, Naini Tal. The CCD observations of the M31 were started in November 1998 using a 1024×1024 pixel² CCD covering $\sim 6' \times 6'$ field. A large size CCD containing 2048×2048 pixel² covering an area of $\sim 13' \times 13'$ was used for the observations in later years. The target field ($\alpha_{2000} = 0^h 43^m 38^s$ and $\delta_{2000} = +41^\circ 09'.1$) is centered at a distance of about 15 arcmin away from the center of M31. The detailed overview of telescope and instruments are given in paper I. A brief summary of the characteristic parameters of the two CCDs used for observations are given in Table 1. To minimize air mass effects, most of the observations were taken when zenith distance was ≤ 3 hour. We

Send offprint requests to: Y. C. Joshi,
e-mail: yogesh@upso.ernet.in

Table 1 Characteristic parameters of the two CCDs used for observations.

Size of CCD (pixel ²)	Field (arcmin ²)	Quantum Efficiency R(%)	Efficiency I(%)	Gain (e ⁻ /ADU)	Readout Noise (e ⁻)	Pixel size (arcsec)
1024 × 1024	~ 6 × 6	35	31	2.96	4.1	~0.37
2048 × 2048	~ 13 × 13	74	61	10.00	5.3	~0.37

have accumulated 468 and 383 data points in *R* and *I* filters respectively during 141 observational nights spanning over ~1200 days. Table 2, available electronically either from authors or at the CDS, lists the date of observation, corresponding Julian date and total exposure time. The average seeing during the entire observing runs was ~2 arcsec.

Data reduction have been performed using the MIDAS and IRAF softwares. Preliminary steps of the image processing include bias and flat fielding corrections. As the dark current during the maximum exposure time of a frame is negligible, it has not been corrected. The cosmic rays contaminations were removed independently from each frame.

The observations were performed in unbinned (0.37×0.37 arcsec²) as well as in 2×2 binned (0.74×0.74 arcsec²) mode during different runs of observations. As the main aim of our observations is to search microlensing events in a combined data of Naini Tal (NTL) and AGAPE (observed with 1.3m MDM telescope at Kitt peak, Arizona, a detailed discussions is given in Calchi Novati et al. 2002), we aligned all the NTL images with respect to a MDM reference image. The NTL images were scaled down or up to MDM pixel size (0.5×0.5 arcsec²). These aligned images, in combination with AGAPE observations, will be used to search for microlensing events using the pixel method described in detail by Ansari et al. (1997).

3. Photometry

To check whether profile fitting photometry could be carried out on the modified NTL images, we compared the photometries carried out on original image and on modified images and the results of a particular night are displayed in Fig. 1. The comparison shows good agreement between the magnitude derived from original and modified images. Therefore we carried out photometry on the modified images. In order to increase signal to noise ratio, all the images of a night were stacked together resulting one frame per filter per night. This then provides us 133 *R* and 166 *I* data points which were used in further analysis.

Using DAOPHOT ‘FIND’ routine, we identified ~4400 resolved stars in the reference frame at 4σ detection level. Stellar photometry for all the images in both filters has been carried out for these resolved stars in ‘fixed-position mode’ using DAOPHOT photometry as described by Stetson (1987). PSF was obtained for each frame using 25-30 uncontaminated stars. DAOPHOT/ALLSTAR (Stetson 1987) routine was used to calculate the instrumental magnitude of the detected stars for each individual frame. The internal errors estimated from the S/N ratio of

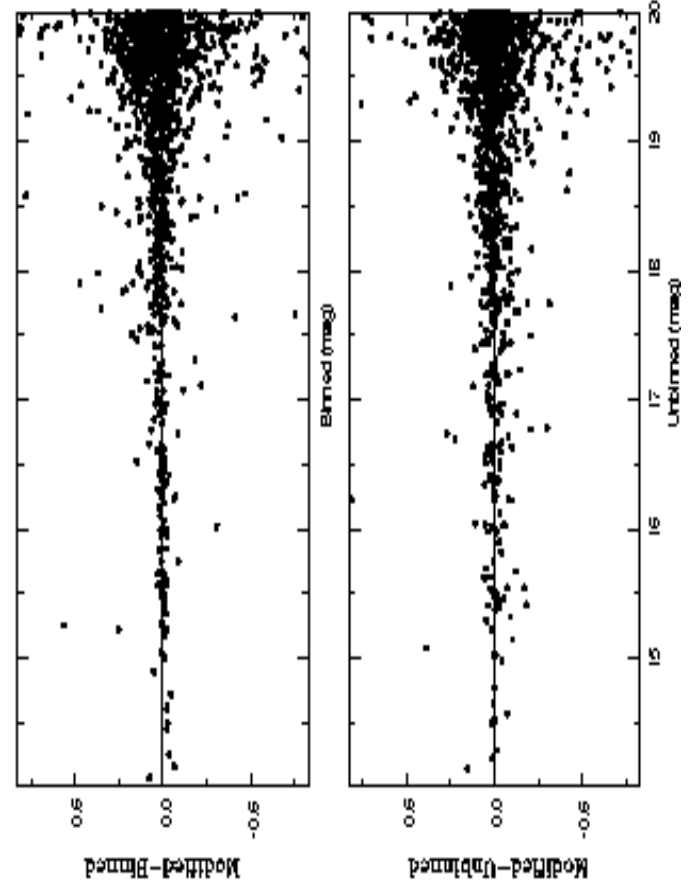


Fig. 1. The plot shows difference in photometries carried out on original and modified images as a function of magnitude. In the upper panel original pixel size (0.74 arcsec) was scaled down (0.5 arcsec), whereas in the lower panel the pixel size (0.37 arcsec) was scaled up (0.5 arcsec).

the stars as output of the ALLSTAR are given in Table 3 as a function of brightness. The error become large (> 0.1 mag) for stars fainter than $R \sim 20.0$ mag.

Table 3 Internal photometric errors as a function of brightness. σ is the standard deviation per observation in magnitude.

Magnitude range	σ_R	σ_I
≤ 14.0	0.01	0.01
14.0 - 15.0	0.01	0.01
15.0 - 16.0	0.01	0.01
16.0 - 17.0	0.01	0.02
17.0 - 18.0	0.02	0.04
18.0 - 19.0	0.04	0.06
19.0 - 20.0	0.07	0.13
20.0 - 21.0	0.15	0.33

3.1. Photometric Calibration

The absolute calibration has been done using Landolt’s (1992) standard field SA98 observed on a good photometric night of 25/26 October, 2000. The airmass ranges from 1.3 to 2.1 during the observations. Atmospheric extinction coefficients determined from these observations are 0.11 ± 0.01 and 0.08 ± 0.01 mag/airmass in R and I filters and they have been used in further analysis. Thirteen standard stars having range in brightness ($11.95 < V < 15.84$) and colour ($0.09 < (R - I) < 1.00$) were used to derive following transformation equations.

$$\Delta(R - I) = (0.96 \pm 0.01) \times \Delta(r - i) \quad (1)$$

$$\Delta(R - r) = (0.03 \pm 0.03) \times (R - I) \quad (2)$$

where R and I are the Landolt standard magnitudes while r and i are the corresponding instrumental magnitudes. The zero point errors are about 0.02 mag in R and 0.01 mag in $(R - I)$. Equations (1) and (2) were used to generate 50 secondary standards in the target field observed on the same night by accounting the differences in exposure times and air-masses. To standardize the remaining stars, differential photometry has been performed with these secondary stars rejecting those which were showing more than 3σ deviation. This process yields an accuracy of 0.03 mag in zero points. A variation of ± 0.1 mag was found around the mean value in the secondary stars itself during the whole observing runs which can be treated as an accuracy in NTL photometry.

3.2. Comparison with the previous photometries

A comparison of the present I band data with those available in the literature (Magnier et al. 1992, Mochejska et al. 2001 for the DIRECT collaboration) has been shown in Fig. 2 as it is the only common filter. An offset of 0.13 mag is observed between our and Mochejska et al. (2001) I band photometry while a difference with Magnier et al. (1992) data indicates a magnitude dependence with a slope of 0.02. A similar slope is seen between Mochejska (2001) and Magnier et al. (1992) data. These results suggest that Magnier et al. (1992) data is colour dependent while Mochejska et al. (2001) data has zero point offset.

4. Detection of variable stars

4.1. Selection Criteria

We do not have all the observations in good photometric sky conditions. Therefore we have rejected all those data points showing photometric error of > 0.2 mag. Further, for each star, the average DAOPHOT error and its standard deviation was calculated using its observations on different nights. Measurements with errors exceeding to average error by more than 3σ were flagged as ‘bad’ and removed from further analysis. The whole procedure was iterated thrice. Normally 1 to 10 points were removed in

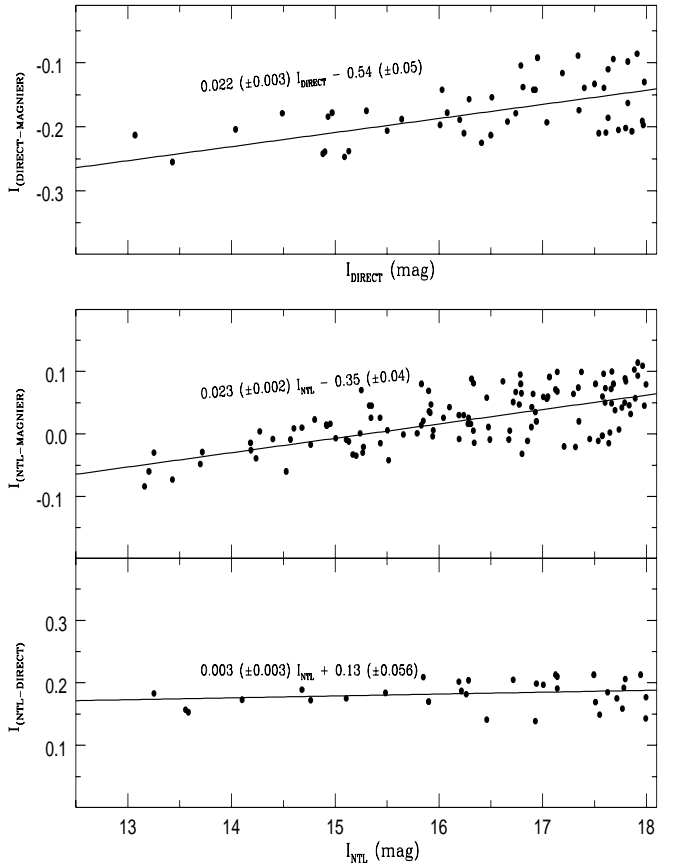


Fig. 2. Comparison of the present I band CCD photometry with those given by Magnier et al. (1992) and Mochejska et al. (2001).

this process. Because two different CCDs with different quantum efficiencies (see Table 1) and different exposure times (see Table 2) were used, limiting magnitudes were different in different years. Consequently some stars could not be identified in one or other years of observations. All the stars were not present in every frame due to different observing conditions and CCD orientations on various nights. In order to derive useful results, we consider only those stars in our further analysis which have more than 40 R data points. Stars which were showing more than 5σ variation in 3 consecutive data points are searched for variability. Only R band photometric data is used for this as the data sample in R filter (133) is larger than that in I filter (116). Also photometric errors at a given brightness are generally less in R filter (see Table 3). Finally we analysed the variability in these stars explicitly by visual monitoring and also using I filter data. In this way, we detected 359 variable stars in our field.

4.2. Period determination

To find periods from unequally spaced data, we used a modified version of the period-searching program by Press and Rybici (1989) based on the method of Horne

& Baliunas (1986). The data were initially phased for all periods between 5 and 600 days searched in an increment step of 0.6 day. To further refine the period, an increment of 0.1 day was used around thus derived period. In this way, we could determine period of 141 variables. The remaining stars are either non-periodic or long-period variables.

4.3. Mean magnitude

We calculated phase weighted apparent mean magnitude for all the Cepheid variables as suggested by Saha et al. (1994)

$$\bar{m} = -2.5 \log_{10} \sum_{i=1}^n 0.5(\phi_{i+1} - \phi_{i-1}) 10^{-0.4m_i}$$

where n is the total number of observations, ϕ_i is the phase of i^{th} observation in order of increasing phase after folding the period. The equation requires non-existent entities ϕ_0 and ϕ_{n+1} which is set identical to ϕ_n and ϕ_1 respectively. The estimation of mean magnitude by the phase-weighted method is superior to an ordinary mean, which minimizes the systematic biases from loss of faint measurements in the mean magnitude (Saha & Hoessel 1990). For other variables, mean magnitude is estimated simply by intensity averaging of all the data points.

4.4. Astrometry

Transformation equations were derived to convert pixel coordinates (X,Y) into celestial coordinates (α_{2000} , δ_{2000}) using 324 reference star positions from the USNO¹ catalogue. These coordinates agree within ~ 0.1 arcsec with those given in Magnier catalogue (Magnier et al. 1992).

5. Cepheid Variables

Cepheid variables are post-main sequence stars occupying the instability strip in H-R diagram. Their light curves display the characteristic ‘sawtooth’ pattern, with periods ranging from a few days to more than 100 days. We have identified 26 Cepheid variables in the disk of M31 (Fig. 3). The Cepheids were identified by looking for the stars with light curves similar in appearances to known Cepheids of M31. The period of the Cepheids was determined as described in Sect. 4.2. The periods estimated independently in two filters agree very well for most of the Cepheids; however difference in the period exists for a few short period variables due to their low amplitude as well as comparatively larger photometric error in I -band. Therefore, the period calculated using R filter data was considered as the period of the star and phase in both R and I filters have been evaluated using this period.

Since most of the Cepheids are believed to be in their second crossing of the instability strip, their period of pulsation is directly related to the stellar mass, and hence,

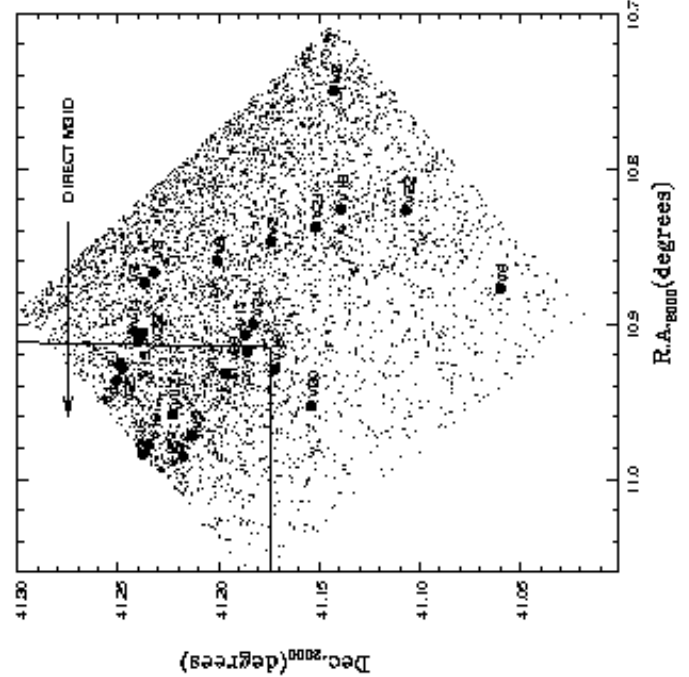


Fig. 3. Location of the 26 Cepheids identified in our data juxtaposed over the entire observed field of M31. Small dots indicates the position of 4400 stars observed in our field. Overlapping area of DIRECT M31D field is also shown.

to the main sequence life time of the star. Hence a rough estimate of the age of the star can be obtained from the observed pulsation period of the Cepheids. We have used the following relation given by Magnier et al. (1997b) to estimate the age of Cepheids:

$$\log A = 8.4 - 0.6 \log P \quad (3)$$

where A is the age of the Cepheid in years and P is the pulsation period in days. As Cepheids detected in our study have period ranging from ~ 7.5 to 56 days, the age of the Cepheids varies from ~ 22 to 75 Myrs with a peak of 48 Myrs. Though there is an uncertainty of ± 0.15 in $\log A$ (Magnier et al. 1997b), this relation provides an indicative age of the Cepheids in M31, and hence some idea of the recent star formation history in the field of our observations.

In Table 4, we present characteristics of these 26 Cepheid variables detected in our study. The identification number of the star, celestial coordinate for J2000, phase weighted mean magnitude in both R and I filters, amplitude of variability in R filter, period, age of the Cepheid (estimated using Eq. 3) and total number of points in R filter used for the light curve study are given. The Cepheids are sorted in the increasing order of their periods. The reference to variability reported in the literature and corresponding period, if known, are listed in the last two columns. Out of the catalogued 26 Cepheids, the variability is being reported for the first time for stars V22 and V24; moreover 13 of the variables are identified

¹ United State Naval Observatory

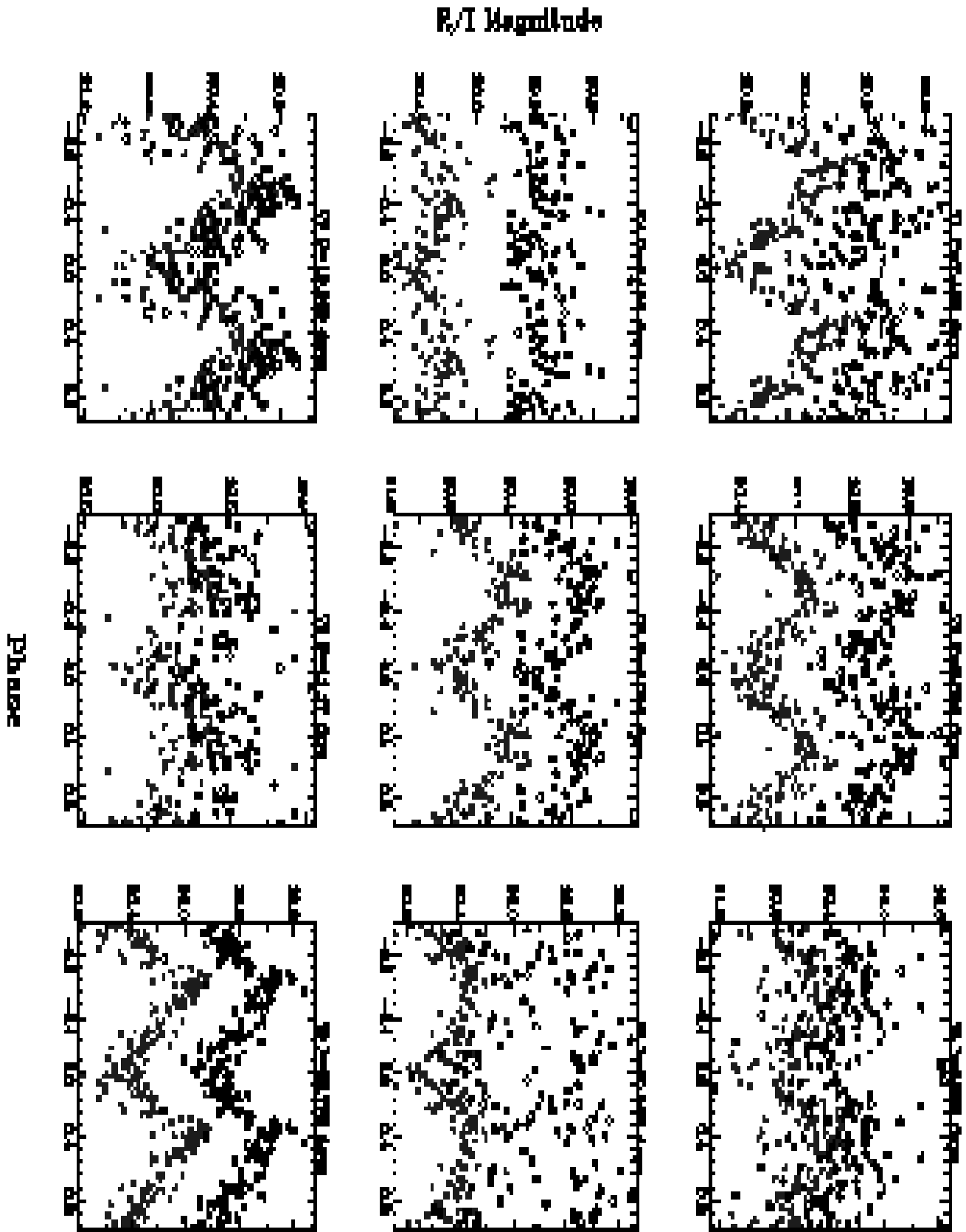
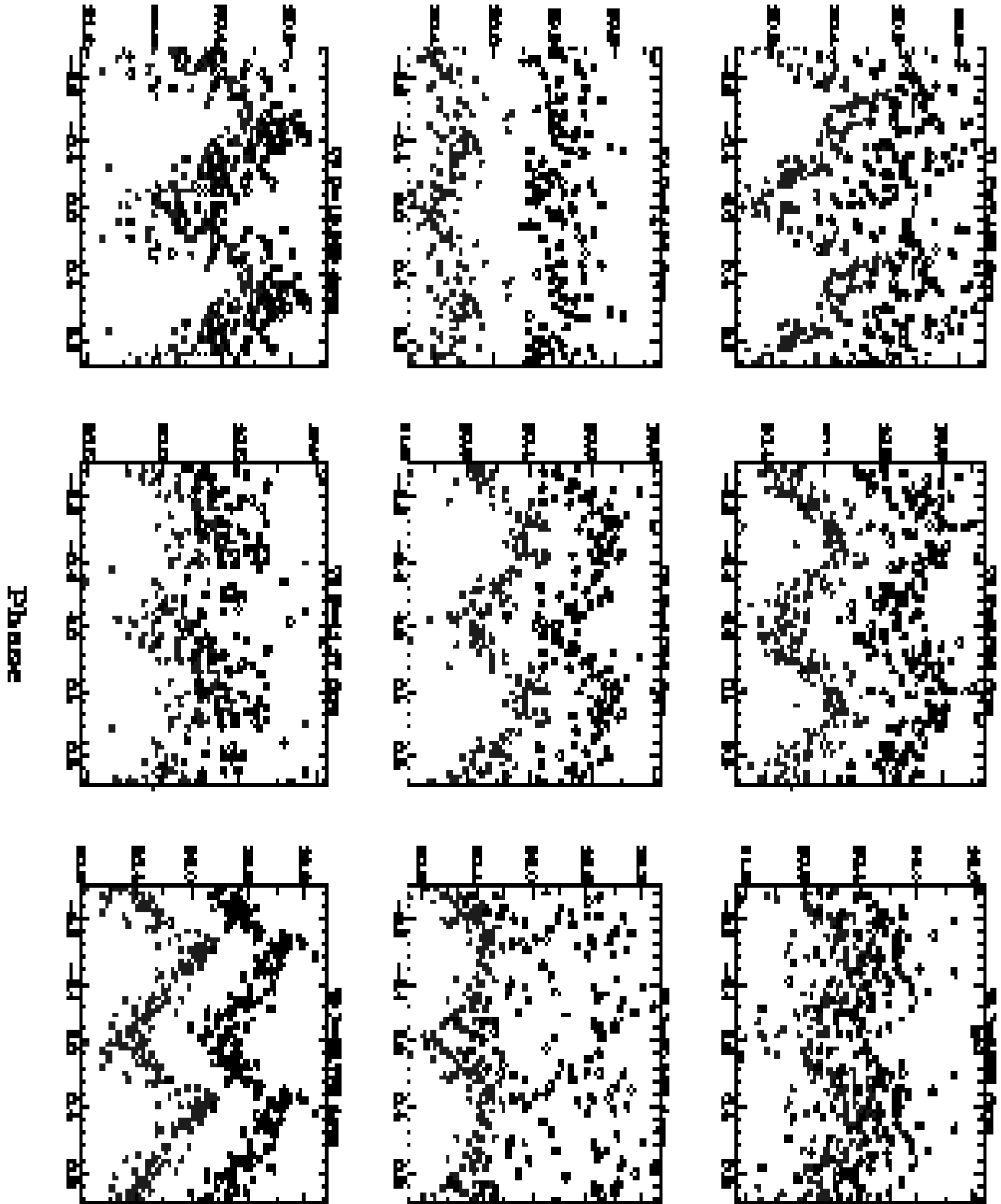
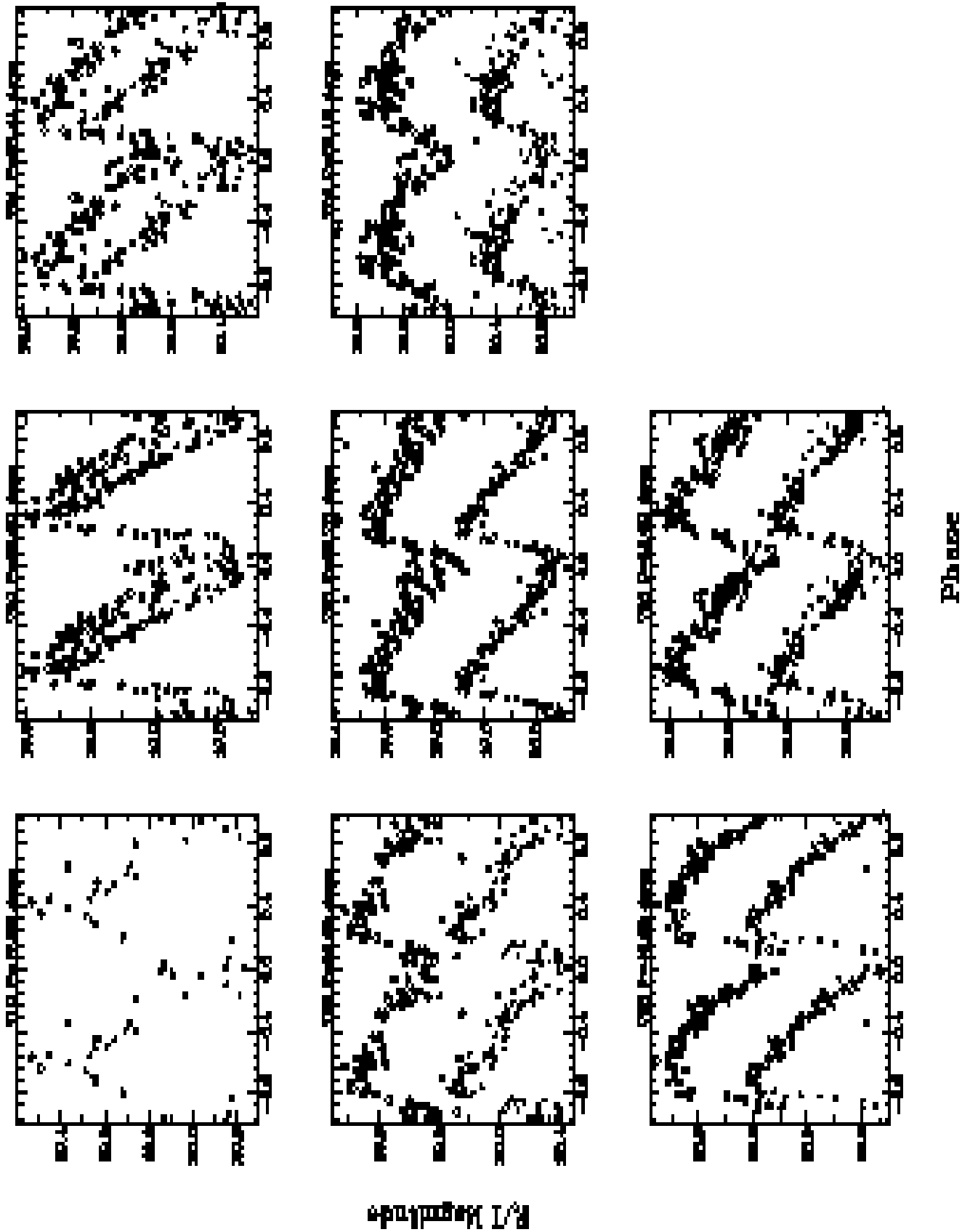


Fig. 4. Phase-magnitude diagram is plotted for 26 Cepheids detected in the present study. Filled and open circles represents R and I magnitudes respectively.

F/I Magnitude

continued...



continued...

Tbale 4. A list of 26 Cepheids observed in our study with their characteristic parameters. Star identification by KAL99, Tomaney & Crotts (1996), MAG97 and Berkhuijsen, E. M. et al. (1988) are prefixed with K, TC, M and B respectively in column 10. The periods of the 13 Cepheids given in the catalogues are given in the last column. The Cepheids discovered and classified by us are marked as † and * respectively in the first column.

Star ID	α (deg)	δ (deg)	\bar{R} (mag)	\bar{I} (mag)	Δ_R (mag)	Period (days)	Age (Myrs)	N	Other Identification	Period (days)
V1	10.9321	41.1970	20.48	19.98	0.27	7.459±0.002	75	123	K V883	7.459
V2*	10.8469	41.1737	20.17	19.69	0.15	8.566±0.003	69	124	TC 170	—
V3*	10.8669	41.2320	20.61	20.28	0.22	8.836±0.004	68	120	TC 18	—
V4	10.9366	41.2503	20.28	19.54	0.11	9.160±0.008	67	86	K V1219	9.173
V5	10.9721	41.2128	20.56	20.04	0.19	9.790±0.005	64	92	K V2879	9.790
V6*	10.8770	41.0601	20.43	19.76	0.15	10.383±0.009	62	93	TC 76	—
V7*	10.8736	41.2367	20.42	20.27	0.28	10.500±0.004	61	123	TC 16	—
V8	10.7500	41.1426	19.89	19.55	0.17	11.17 ±0.01	59	95	M 65	25.0±5.0
V9*	10.8594	41.2004	20.21	19.60	0.26	13.773±0.006	52	126	TC 20	—
V10*	10.9290	41.1715	20.77	19.84	0.48	14.420±0.006	51	116	TC 85	—
V11	10.9255	41.2489	19.57	18.87	0.16	15.26 ±0.01	49	96	K V635	15.255
V12	10.9576	41.2227	20.84	20.08	0.32	15.46 ±0.01	49	89	K V2286	15.464
V13	10.8259	41.1386	19.82	19.46	0.40	15.76 ±0.01	48	94	M 68	14.0±2.8
V14*	10.9049	41.2419	19.93	19.58	0.22	15.90 ±0.01	48	121	TC 194	—
V15*	10.9115	41.2396	20.79	19.91	0.30	15.95 ±0.01	48	126	TC 196	—
V16	10.9775	41.2348	20.28	19.74	0.40	16.38 ±0.02	47	47	K V3198	16.345
V17*	10.9069	41.1868	20.12	19.60	0.39	16.60 ±0.01	47	124	B 4614	—
V18	10.9853	41.2176	19.47	19.09	0.21	17.73 ±0.01	45	91	K V3583	17.703
V19	10.9839	41.2374	19.83	19.60	0.32	17.83 ±0.03	45	18	K V3551	16.699
V20*	10.9526	41.1540	19.20	18.99	0.35	20.09 ±0.01	42	96	TC 207	—
V21	10.8379	41.1514	19.74	19.31	0.39	21.44 ±0.02	40	96	M 69	13.0±2.6
V22†	10.8272	41.1071	20.01	19.19	0.29	26.99 ±0.04	35	92	—	—
V23*	10.9059	41.2379	19.78	18.92	0.34	28.78 ±0.02	33	127	TC 30	—
V24†	10.9002	41.1823	20.55	19.57	0.23	35.12 ±0.05	30	121	—	—
V25	10.9293	41.2475	18.89	18.35	0.31	43.53 ±0.08	26	97	K V836	43.371
V26	10.9183	41.1856	19.36	18.82	0.22	56.02 ±0.08	22	124	K V164	56.116

as Cepheids for the first time. The remaining 13 Cepheids have been known from earlier studies. The present data confirms their variability and our periods are generally in good agreement with the reported value.

In Fig. 4, we show the phase-magnitude diagram for all the 26 Cepheids in both R and I filters. The I -band light curves show more scattering particularly for short period and low amplitude Cepheids. This could arise due to the following reason: the amplitude of Cepheids decreases with increasing wavelength (e.g. Freedman et al. 1985) and Freedman (1988) found a ratio of 1.00:0.67:0.44:0.34 in amplitudes of $B:V:R:I$ filters. As most of these Cepheids have pulsation of ~ 0.1 - 0.2 magnitude in R filter, the amplitude of pulsation in I filter is even less and becomes comparable to the photometric errors.

5.1. Comparison with earlier studies

Our target field in M31 has been observed only in a few earlier surveys. The V band photometric observations have been obtained by Magnier et al. (1997a, hereafter referred to as MAG97) for about 25 days. They have observed 9 fields of M31 and each field covered a region of $\sim 11 \times 11$ arcmin² on the sky. They found 130 Cepheids

in the survey. As we have observed smaller field, only 3 of them are located in our field and we have identified all of them. In Table 4, we have compared period of these stars with those found in our data set. One can easily notice a large discrepancy between the periods obtained in two surveys which we attribute to insufficient observations by MAG97.

BVI photometry has been carried out by Kaluzny et al. (1999, hereafter referred to as KAL99) under the DIRECT project. Out of 35 Cepheids detected in DIRECT project in the field M31D, 11 are located in our field of observations. We have identified 10 of them and notice that except in the case of V19, the periods determined in the two surveys are in excellent agreement. The discrepancy in the period of V19 appears to be due to inadequate data in the present study (see Table 4). One of the Cepheid (K V952) reported in KAL99 could not be detected in our data due to blending effect as this star is highly blended by a neighbouring bright red star.

For Cepheids V7, V9, V14, V15, V17, V23 and V26, the parameters given in Table 4 supersedes our earlier results given in paper I, as these are derived using data with much longer temporal coverage.

5.2. The Period-Luminosity (P-L) Diagram

The Cepheid variables exhibit a stable periodic variability and there is an excellent correlation between their mean intrinsic brightness and pulsation period. Consequently, the Cepheid Period – Luminosity relation provide an important standard candles to measure distances to galaxies up to the Virgo Cluster, by comparison of their absolute magnitudes inferred from P-L relation with their observed apparent magnitudes. Based on the study of Cepheids located in LMC, SMC and IC 1613 galaxies, Udalski et al. (2001) found that the zero points of the P-L relations have no significant dependence on metallicity. In fact, they are constant to within ~ 0.03 mag. However, the values could be affected due to other effects, e.g. blending, which can cause up to 10% uncertainty in the distance determination of M31 (Mochejska et al. 2000). We have therefore used metallicity independent P-L relation in the present analysis.

Using a set of 32 LMC Cepheid variables, Madore & Freedman (1991) have obtained an equation of the ridge line in P-L diagram for Cousin R filter as:

$$M_R = -2.94(\pm 0.09)(\log P - 1) - 4.52(\pm 0.04) \quad (4)$$

while using a large sample of 658 Cepheids, Udalski et al. (1999c) derived a PL relation for Cousin I filter as:

$$M_I = -2.96(\pm 0.02)(\log P - 1) - 4.90(\pm 0.01) \quad (5)$$

where we adopt a true distance modulus of 18.5 mag for the LMC (Freedman et al. 2001) instead of 18.2 mag used by Udalski et al. (1999c).

The apparent mean magnitudes of 26 Cepheids are plotted as a function of $\log P$ in Fig. 5. The slope of the straight line is fixed as -2.94 and -2.96 for R and I filters respectively. The Cepheids V24 and V26 are located by about 1.0-1.5 mag below the ridge line in the P-L diagram which makes them a possible Population II Cepheid variables. Therefore, we did not consider these two Cepheids for the zero points evaluation. Using remaining 24 Cepheids, we found a zero points of 23.54 ± 0.09 and 23.02 ± 0.07 mag in R and I filters respectively. The dashed envelope lines are drawn 0.5 magnitude from the fitted line, representing the expected intrinsic scatter of P-L relation due to the finite width of the instability strip in the H-R diagram (Sandage 1958, Sandage & Tammann 1968), blending of Cepheids as well as the range of interstellar extinction.

The above zero points give us a mean apparent distance modulus of 25.12 ± 0.09 and 24.96 ± 0.07 mag in R and I filters respectively. This yields a mean colour excess of

$$E(R - I) = (m - M)_R - (m - M)_I = 0.16 \text{ mag} \quad (6)$$

Using this and the standard extinction law given by Cardelli et al. (1989), we found a total extinction of 0.63 and 0.47 mag in R and I filters respectively. Correcting the apparent distance modulus for the total extinction, we

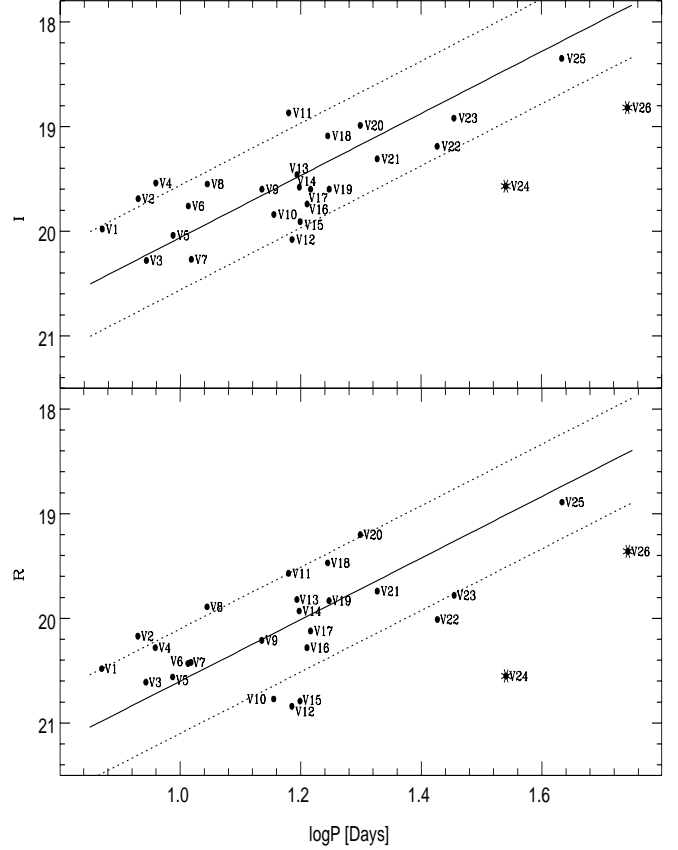


Fig. 5. Period-Luminosity relation for 26 Cepheids observed in our field. Lower panel indicates P-L relation for R filter while upper panel indicates the same for I filter. Filled circle: fundamental mode Cepheids; asterisk: possible Population II Cepheids. No corrections for reddening have been applied to either data set. The slope of the fitted straight lines are fixed at $dm/d \log P = -2.94$ and -2.96 for R and I filters respectively. The dashed envelope lines have been drawn 0.5 magnitude from the straight line fit (see text for details).

obtain a distance modulus of 24.49 ± 0.11 mag for the M31 which corresponds to a distance of 790 ± 45 Kpc. Stanek & Garnovich (1998) based on red clump method and Holland (1998) based on globular cluster CMDs estimated a distance of M31 as 780 Kpc while a recent determination of Freedman et al. (2001) based on Cepheid P-L relation suggest a distance of 750 Kpc for M31. Present estimate of M31 distance is thus agrees well with them.

5.3. The Colour-Magnitude Diagram

In the M_R , $(R - I)_0$ diagram, locations of the Cepheids under discussion are shown (Fig. 6). The isochrones by Bertelli et al. (1994) for solar metallicity drawn for $\log A$ as 7.4 and 7.9 are also plotted which supports the age estimated from equation (5). As most of the detected Cepheids ranges in magnitude from 19 to 21 in R filter

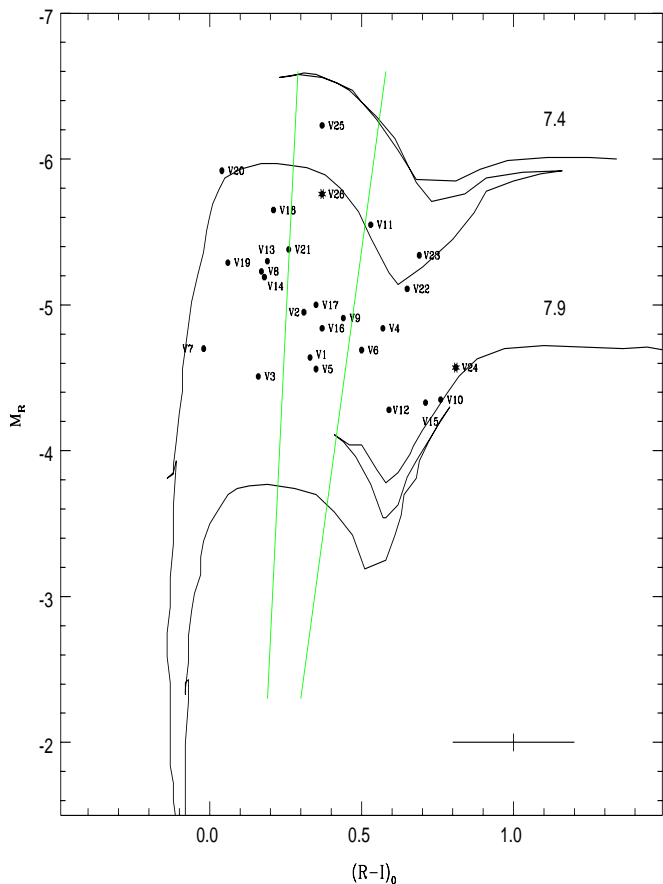


Fig. 6. The colour-magnitude diagram for the Cepheids under discussion. Symbols are the same as in Fig. 7. The solar metallicity isochrones by Bertelli et al. (1994) for $\log A = 7.4$ and 7.9 are also plotted. Average magnitude of errors in observations are shown in the right bottom corner of the figure.

and 18 to 20 in I filter, there can be an error of ~ 0.2 mag in the colour determination.

5.4. Location of the Cepheids

The locations of the Cepheids (see Fig. 3) indicate that most of them are towards the inner side of M31 (bulge direction), where, possibly, the star formation was active a few million years ago. This inference is further supported by the fact that, the early type supergiants detected in our field ($R \sim 16$ to 19 mag) also occupy the same strip where the Cepheids are found. So it is tempting to suggest that we are possibly tracing one of the spiral arms of M31.

5.5. Brief description of the Cepheids

We detect 26 Cepheids in which V22 and V24 are newly discovered while V2, V3, V6, V7, V9, V10, V14, V15, V17, V20 and V23, as reported variables in earlier studies, are identified Cepheids for the first time. Out of the 26 Cepheids, only 12 are monitored for a period of four years

while remaining are observed only for last three years. The period of 4 Cepheids were cross-examined using INT data (obtained with 2.5m telescope at La Palma, Canarie Islands) using Laffer-Kinman (1965) periodogram which agree quite well with our estimated period except V8 which have a low amplitude, highly scattered light curve and needs further investigation. One of the Cepheid, V4, could not be ascribed as a Cepheid variable purely on the basis of our data. However, V band light curve of the same star in KAL99 clearly indicates its Cepheid nature. Other interesting Cepheids are briefly described below:

V19— KAL99 obtained a period of 16.999 days for this Cepheid while we obtained a period of 17.83 ± 0.03 days using 18 data points. The light curve for this Cepheid is extremely under-sampled and poorly distributed in phase in our data which could be the reason for discrepancy between two periods.

V22— It is discovered in the present study with a period of 26.96 ± 0.04 days. A small bump in the falling branch can be seen in both filters.

V24— This is another Cepheid discovered by us. It has a period of 35.12 ± 0.05 days and an exceptionally large value of $(R - I)$ colour of 0.98 mag. In the P-L diagram, this Cepheid deviates maximum towards the fainter side in both filters and could be a possible Population II Cepheid.

V26— This is the longest period Cepheid in our sample. We obtained its period as 56.02 ± 0.08 days in agreement with a period of 56.116 days derived by KAL99. In the P-L diagram, this Cepheid is also located downwards in both filters and it could also be a Population II type Cepheid.

6. Other variables

In addition to the Cepheid variables reported in our field, 333 other variable stars are also found in the present study. Most of them appear to be irregular variables. Only 115 stars are found periodic for which we could determine approximate period and magnitude. In Table 5, available in the electronic form either from authors or at the CDS, we have given the identification number, celestial coordinates, mean magnitude in R and I filters, amplitude variation and nature of these 333 stars in R filter. Out of these 333 stars, 32 were already categorized (see Table 5). V176 and V284 are suspected as a binary and light curve for one of them is shown in Fig 7(a). We have given the light curve of a periodic star V154 with period ~ 236 days in Fig. 7(b) while the light curve of an irregular variable V252 is shown in Fig 7(c).

7. Conclusion

We have been imaged $\sim 13 \times 13$ arcmin² region of the M31 disk for about 4 years during 1998 to 2001 in R and I pass-bands. Using 141 nights of observation spanning a period of ~ 1200 days, we have detected 26 Cepheids among which variability in 2 stars has been found for the first time. We have established the Cepheid nature of 11 variables in the

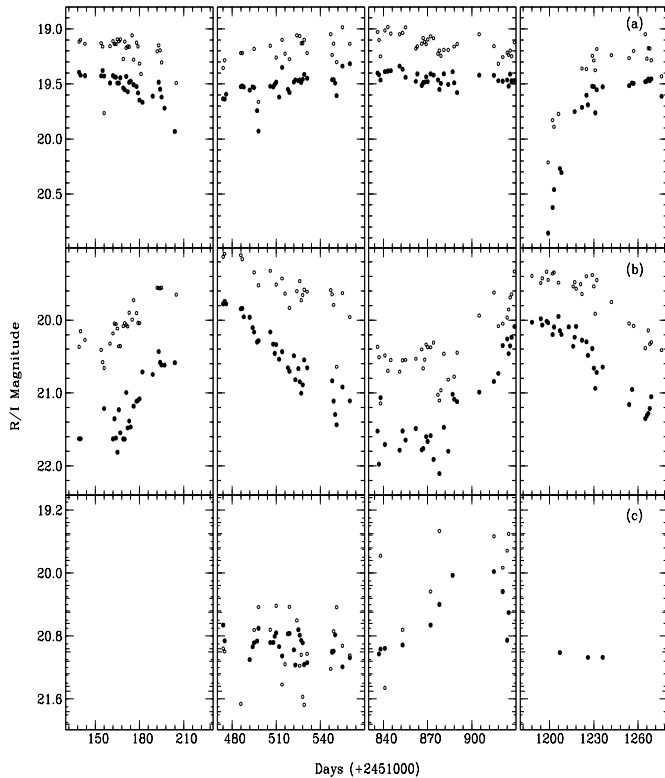


Fig. 7. The typical light curve of 3 other variables (for further detail see Sect. 6). Filled and open circles represent R and I filters respectively.

sample, while we confirm the period and nature of variability in the other 13 stars. The long duration data enabled us to obtain accurate period and mean magnitude of the Cepheids. The period obtained for these Cepheids ranges from ~ 7.5 to 56 days. They range in age from 22 Myrs to 75 Myrs and occupy a strip where the early type supergiants too are located. Using the period-luminosity relation of the Cepheids, we derive a distance of 790 ± 45 Kpc for M31. There could be additional uncertainty in the distance determination due to blending effect in Cepheids as well as variable extinction within the observed region.

In addition to Cepheids, we also detect 333 variable stars. Out of them, 115 are periodic variables, 2 suspected eclipsing binaries and remaining 216 stars appear to be irregular variables.

We have thus demonstrated once more that a meter class telescopes like ours can play important role in the study of variable stars provided large amount of telescope observing time is made available. These data are also valuable for the search of gravitational microlensing events towards M31. We are in the process of identifying lensing candidates in our target field and their detailed study shall be presented in the forthcoming publication.

Acknowledgments We would like to thank the referee Dr. B.J.Mochejska for useful remarks on the manuscript.

We are also thankful to Dr. Vijay Mohan for his helpful advice during observations and Drs. Jean Kaplan, Alan Bouque and Vincenzo Cardone for useful discussions during the course of the work. This study is a part of the project 2404-3 supported by Indo-French center for the Promotion of Advance Research, New Delhi.

References

- Ansari, R., Auriere, M., Baillon, P., et al. 1997, *A&A*, **324**, 843
 Beaulieu, J.P., Grison, P., Tobin, W. et al. 1995, *A&A*, **303**, 137.
 Berkhuijsen, E.M., Humphreys, R.M., Ghigo, F.D., & Zumach, W., 1988, *A&AS*, **76**, 65
 Bertelli, G., Bressan, A., Chiosi, C., Fagotto, F., & Nasi, E., 1994, *A&AS*, **106**, 275
 Calchi Novati, S., Iovane, G., Marino, A.A., et al., 2002, *A&A*, **381**, 848
 Cardelli, J.A., Clayton, G.C. & Mathis, J.S., 1989, *AJ*, **345**, 245
 Crots A.P.S. & Tomaney, A.B., 1996, *ApJ*, **473**, L87
 Freedman, W.L., Grieve, G.R. & Madore, B.F., 1985, *ApJS*, **59**, 311
 Freedman, W.L., 1988, *ApJ*, **326**, 691
 Freedman, W.L., Wilson C.D. & Madore, B.F., 1991, *ApJ*, **372**, 455
 Freedman, W.L., Madore, B.F., Gibson, B.K. et al. 2001, *ApJ*, **553**, 47
 Holand, S., 1998, *AJ*, **115**, 1916
 Horne, J.H., & Baliunas, S.L., 1986, *ApJ*, **302**, 757
 Joshi, Y.C., Pandey, A.K., Narasimha, D. & Sagar, R., 2001, *BASI*, **29**, 531
 Kaluzny, J., Mochejska, B.J., Stanek, K.Z., et al. 1999, *AJ*, **118**, 346
 Lafler, J. & Kinman, T.D., 1965, *ApJS*, **11**, 216.
 Landolt, A.U., 1992, *AJ*, **104**, 340
 Madore, B.F. & Freedman, W.L., 1991, *PASP*, **103**, 933
 Magnier, E.A., Lewin, W.H.G., van Paradijjs, J., et al. 1992, *A&AS*, **96**, 379
 Magnier, E.A., Augusteijn T., Prins, S., van Paradijs, J., & Lewin, W.H.G., 1997a, *A&AS*, **126**, 401
 Magnier, E.A., Prins, S., Augusteijn, T., Paradijjs, J., & Lewin, W.H.G, 1997b, *A&A*, **326**, 442
 Mochejska, B.J., Macri, L.M., Sasselov, D.D. & Stanek, K.Z., 2000, *AJ*, **120**, 810
 Mochejska, B.J., Kaluzny, J., Stanek, & Sasselov, D.D., 2001, *AJ*, **122**, 1383
 Press, W.H., Rybici G.B., 1989, *ApJ*, **338**, 277
 Saha, A. & Hoessel, J.G., 1990, *AJ*, **99**, 97
 Saha, A., Labhardt, L., Schwengeler, H., et al. 1994, *ApJ*, **425**, 14
 Sandage, A., 1958, *ApJ*, **127**, 513
 Sandage, A. & Tammann, G.A., 1968, *ApJ*, **151**, 531
 Stetson, P.B., 1987, *PASP*, **99**, 191
 Stanek, K.Z. & Garnavich, P.M., 1998, *ApJ* **503**, L131
 Tomaney, A.B. & Crots, A.P.S., 1996, *AJ*, **112**, 2872
 Udalski, A., Soszynski, I., Szymanski, M., et al. 1999a, *Acta Astrono.*, **49**, 45
 Udalski, A., Soszynski, I., Szymanski, M., et al. 1999b, *Acta Astrono.*, **49**, 437
 Udalski, A., Szymanski, M., Kubiak, M., et al. 1999c, *Acta Astrono.*, **49**, 201

- Udalski, A., Wyrzykowski, L., Pietrzyński, G., et al. 2001, *Acta Astrono.*, **51** 221
- Welch, D.L., Alcock, C., Allsman, R. A., et al. 1997, in *Variable Stars and the Astrophysical Returns of Microlensing Surveys*, ed. R. Ferlet, J. P. Maillard, & B. Raban (Editions Frontieres), 205